Published in final edited form as:

ACS Appl Bio Mater. 2020 June 15; 3(6): 3914–3922. doi:10.1021/acsabm.0c00466.

Experimental Single-Platform Approach to Enhance the Functionalization of Magnetically Targetable Cells

Mark R. Battig[1], **Ivan S Alferiev**[1], **David T. Guerrero**[1], **Ilia Fishbein**[1], **Benjamin B. Pressly**[1], **Robert J. Levy**[1], **Michael Chorny**[1,*]

[1]Department of Pediatrics, The Children's Hospital of Philadelphia, Philadelphia, PA 19104, USA

Abstract

Magnetic guidance shows promise as a strategy for improving the delivery and performance of cell therapeutics. However, clinical translation of magnetically guided cell therapy requires cell functionalization protocols that provide adequate magnetic properties in balance with unaltered cell viability and biological function. Existing methodologies for characterizing cells functionalized with magnetic nanoparticles (MNP) produce aggregate results, both distorted and unable to reflect variability in either magnetic or biological properties within a preparation. In the present study, we developed an inverted-plate assay allowing determination of these characteristics using a single-platform approach, and applied this method for a comparative analysis of two loading protocols providing highly uniform *vs.* uneven MNP distribution across cells. MNP uptake patterns remarkably different between the two protocols were first shown by fluorimetry carried out in a well-scan mode on endothelial cells (EC) loaded with BODIPY558/568-labeled MNP. Using the inverted-plate assay we next demonstrated that, in stark contrast to unevenly loaded cells, more than 50% of uniformly functionalized EC were captured within 5 min over a broad range of MNP doses. Furthermore, magnetically captured cells exhibited unaltered viability, substrate attachment, and proliferation rates. Conducted in parallel, magnetophoretic mobility studies corroborated the markedly superior guidance capacity of uniformly functionalized cells, confirming substantially faster cell capture kinetics on a clinically relevant time scale. Taken together, these results emphasize the importance of optimizing cell preparation protocols with regard to loading uniformity as key to efficient site-specific delivery, engraftment, and expansion of the functionalized cells, essential for both improving performance and facilitating translation of targeted cell therapeutics.

Table of Contents

[*]Corresponding author: Michael Chorny, Ph.D., The Children's Hospital of Philadelphia, Abramson Research Building, Suite 702, 3615 Civic Center Boulevard, Philadelphia, PA 19104-4318; chorny@email.chop.edu, tel: (215) 590 3063, fax: (215) 590 5454.

Supporting Information:

This material is available free of charge *via* the Internet at http://pubs.acs.org.

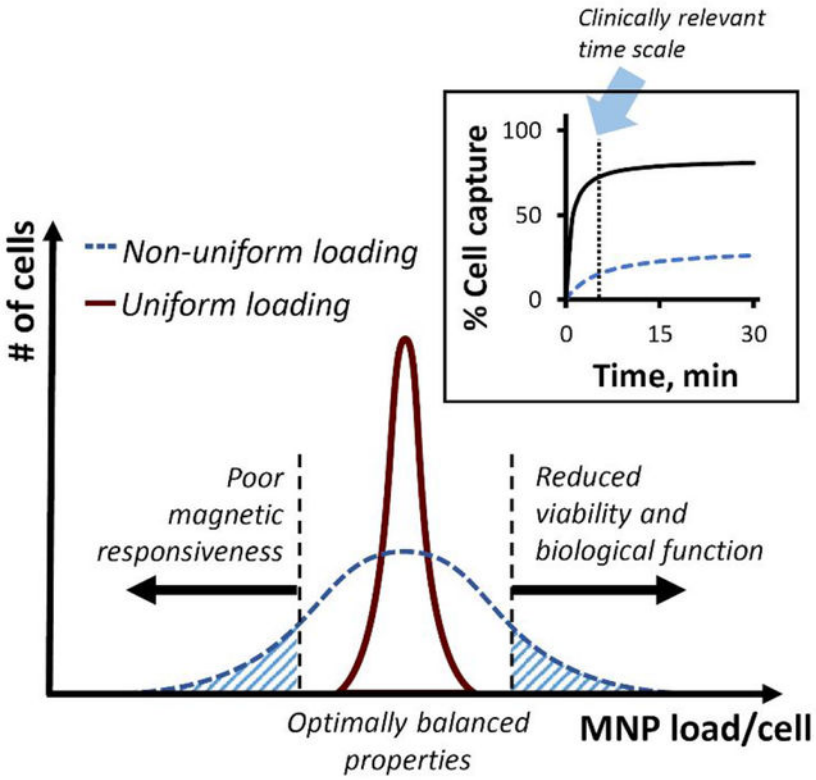

Keywords

magnetic targeting; cell delivery; magnetic nanoparticle; cell functionalization; single-platform assay; endothelial cells

Introduction

Experimental therapies using autologous cells to regenerate damaged tissues and restore normal autocrine and paracrine signaling can pave the way to achieving clinically meaningful improvements in the management of diseases currently lacking effective treatment options.[1] However, in order to realize the clinical potential of cell therapeutics, there is a requirement to develop improved delivery strategies capable of overcoming inefficient homing and poor integration and survival of administered cells at their target sites.[2–4] Major improvements in delivery specificity, cell viability, and biological function are needed for the successful translation and implementation of new cell therapies in clinical practice.[5]

Targeted delivery of cells rendered responsive to magnetic guidance *via* functionalization with iron oxide-containing, magnetizable nanoparticles (MNP) is emerging as an effective approach for achieving site-specific cell homing and engraftment, potentially applicable for treating a broad variety of conditions.[6–10] In the context of cell therapy, magnetic guidance is unique in its ability to actively direct and control the motion, localization, and retention of cells within the target region. However, despite considerable progress in optimizing

magnetic targeting schemes and MNP formulations with respect to their magnetic properties and biocompatibility,[10–13] preclinical testing results suggest that magnetic guidance often fails to substantially improve cell delivery and to provide lasting local cell presence, engraftment, and expansion, all of which essential for realizing the expected therapeutic benefit.[14–15] The lack of consistent improvements in site-specific cell delivery with magnetic guidance emphasizes the importance of identifying critical variables in cell functionalization protocols, in turn posing the need to design more robust and reliable *in vitro* methodologies for evaluating magnetically responsive cell preparations, as a step preceding their further testing in models of human disease.

Effectiveness of cell functionalization for magnetically targeted delivery derives from a balance between adequate magnetic responsiveness and fully preserved cell viability and biological function. This balanced cell functionalization requires protocols that consistently achieve uniform MNP loading throughout the entire cell preparation. In practice, several studies have shown that significant variability in the distribution of the MNP payload arises when loading procedures are poorly adjusted for a specific type of MNP and cells to be functionalized.[16–17] Inadequate functionalization is often evidenced by a sizeable fraction of cells containing no detectable MNP and by highly variable amounts of internalized MNP divided between the remaining cells. The uneven distribution of MNP results in a significant proportion of underloaded cells whose magnetic responsiveness is insufficient for guided delivery.[17–18] It also often increases the fraction of cells overloaded with MNP, thereby reducing capacity for stable substrate binding and expansion,[19–20] and adversely affecting the quality and performance of the cell product (shown schematically in Figure 1). However, the development of improved protocols minimizing MNP uptake variability while preserving the balance between magnetic properties and cell functionality is limited by the availability of reliable analytical methods for determining adequacy and uniformity of cell functionalization. While existing techniques can quickly provide cumulative estimates of several parameters related to the utility of MNP-loaded cell preparations, these properties are typically expressed as an aggregate value for an entire population rather than individual cells or cell fractions. As a result, the magnetic characteristics obtained by these methodologies primarily reflect those of the most highly loaded cells in a sample, which in turn are likely to experience the strongest MNP-related toxicity and show the lowest regenerative potential. Accordingly, cells with the smallest MNP content and thus with the least affected biological function will contribute to a greater degree to the outcomes of the standard cell proliferation and viability assays. Therefore, the results of the both types of measurements are often “favorably” skewed by the respective cell fractions, which may indeed be the least useable (and, in fact, detrimental by adding to the adverse effects) for magnetically guided cell delivery and therapy, prompting erroneous conclusions about both the suitability of a cell functionalization protocol and the quality of a cell preparation. Measurements of MNP loading and magnetic responsiveness carried out separately from the analyses of cell viability, substrate binding, and proliferation rates using cell samples processed in a different way for each set of tests constitutes an additional source of error, as no tools presently exist for determining these properties in parallel, using a simple and reliable single-platform approach.

Focusing on magnetically accelerated reendothelialization of injured blood vessels, our group has designed and characterized biodegradable, poly(lactide)-based MNP that can be rapidly loaded into endothelial cells (EC) through magnetically facilitated endocytosis in amounts sufficient to impart strong magnetic responsiveness without impeding normal cell behavior and functions.[21] By promoting recovery of the disrupted endothelium, magnetically enhanced delivery of autologous EC has the potential to prevent pathological sequelae of arterial injury inevitably associated with vascular intervention procedures. In animal model experiments, magnetic guidance of MNP-functionalized EC using a two-source scheme potentially applicable to non-superficially located targets in the human body[22] resulted in markedly improved site-specificity, lasting presence, and expansion of the administered cells in stented rat carotid arteries.[6] In the present study, we characterized our cell preparation protocol based on the magnetically facilitated endocytosis process with respect to the effectiveness and uniformity of cell functionalization. Using a new single-platform approach (inverted-plate assay), we sought to identify relevant protocol variables and to establish criteria for optimizing the performance of MNP-functionalized cells for targeted delivery applications. Using the original cell loading protocol[6, 21] and an auxiliary procedure designed to experimentally reproduce the characteristic pattern of non-uniform MNP uptake, we comparatively examined the effects of MNP loading variables on cell functionality and capture efficiencies under conditions modeling magnetically guided delivery in the presence of an opposing force. As a simple and robust *in vitro* tool for screening magnetically targetable cells, the inverted-plate assay is expected to assist with identifying effective cell functionalization strategies and facilitate *in vivo* evaluation of experimental cell therapeutics, expediting translation of magnetically targeted cell delivery into the clinic.

Results and Discussion

Identifying and optimizing key parameters in the cell functionalization process are essential for improving the performance of magnetic cell guidance strategies and establishing them as effective and well-characterized tools for targeted delivery of cell therapeutics. An inverted-plate assay designed in this study as a single-platform approach for optimizing the cell functionalization process was first evaluated experimentally for its specificity and accuracy using EC functionalized with biodegradable MNP.[6, 21] Polylactide-based superparamagnetic MNP with a narrow size distribution (290±8 nm, polydispersity index = 0.09) and high magnetic susceptibility exhibit rapid and dose-effective uptake, resulting in near-complete internalization of the particle payload within 24 hr *via* magnetically facilitated endocytosis.[21] As part of the inverted-plate assay validation, bovine aortic EC loaded with MNP (5 μg/well) were combined at predetermined ratios with unloaded cells and placed together as a mixed cell suspension in wells of a 96-well plate. The plate positioned on a permanent magnet was turned over for 30 min to expose the cells to a high-gradient magnetic field (average field gradient of 32.5 T/m) applied against gravity. Fractional capture efficiency of the cells in the presence of the opposing (gravitational) force was found to accurately match the proportion of MNP-loaded EC (Figures S1A, Figure 2A), confirming high selectivity of the assay. Remarkably, within 30 min of exposure to the upwardly directed magnetic force, all the magnetically responsive cells stably adhered and started spreading on the substrate, and fully reassumed normal EC morphology within 3 hr (Figure 2B). In contrast, virtually

all EC in the mixed cell suspension, regardless of the loaded-to-nonloaded cell ratio, adhered to the substrate within 30 min in a plate positioned upright as a control. Conversely, no cell attachment was observed if the plate was kept inverted in the absence of magnetic exposure, confirming that cell capture and stable binding in the inverted-plate setup was conditioned upon the presence of the high-gradient field together with magnetic responsiveness of the cells sufficient to resist gravity (Figure S1A). Notably, the metabolic activity of the captured EC determined using the resazurin/resorufin (Alamar Blue[23]) system was independent of MNP loading. The results of the Alamar Blue measurements agreed with the numbers of captured cells at all tested ratios (R^2 = 0.99), demonstrating the utility of this analytical method for the rapid quantification of EC capture as part of the inverted-plate assay and confirming a lack of short-term adverse effects resulting from the functionalization process (Figures 2A & S1D). Furthermore, Alamar Blue measurements and cell counting performed longitudinally on magnetically captured cells (initial cell density of 1,400 EC per well) showed division rates similar to those of unloaded EC included as a control, with cell numbers increasing 3.95±0.06 and 3.62±0.01 fold a day, respectively, during the exponential growth phase (Figure 2C). Based on these results, cell functionalization required for rapid and selective magnetic cell capture was accomplished using the optimized protocol without altering normal cell behavior or having delayed adverse effects on their proliferation potential. Magnetically guided cells rapidly and stably attached to the substrate and, after a short lag, expanded with exponential kinetics exhibiting a doubling time of 12.1±0.1 hr. Taken together, these findings are consistent with effective targeted delivery, retention and subsequent rapid expansion of MNP-functionalized EC guided to stented arteries using the two-source magnetic targeting strategy,[6] supporting the relevance of the inverted-plate studies to the experimental settings of *in vivo* magnetic cell delivery testing in a preclinical model.

Having established the applicability of the inverted-plate assay for the concomitant characterization of magnetic responsiveness, substrate binding, and proliferation of MNP-functionalized cells, we focused on the effects of the MNP distribution pattern within a cell preparation. To comparatively investigate the role of loading uniformity as a determinant of the magnetic and biological properties of MNP-functionalized cells, the cell functionalization step was modified to simulate the result of a loading process causing uneven distribution of the particle payload across the cells.[17–18] MNP stably labeled with a biocompatible red fluorescent dye of the boron dipyrromethene series[24] ($BODIPY_{558/568}$) were formulated for these experiments as reported previously.[25] In contrast to the optimized loading procedure resulting in EC evenly loaded with MNP at all tested doses as shown by fluorescent microscopy and by live cell fluorimetry applied in a well-scan mode (Figure 3A–B, Figure S2), the modified protocol closely recapitulated the characteristics of a non-uniform loading process[17, 26–27], causing the majority of the particle payload to primarily be distributed between a limited number of cells, with a significant proportion of EC showing little or no MNP-associated fluorescence even at the highest tested particle dose of 10 μg/well (Figure 3A–B). Besides marked differences in the correlation between the cell-associated fluorescent signals and the corresponding MNP doses (excellent and poor, respectively, for the optimized and simulated non-uniform loading procedures, Figure S2A), the relative standard deviations (RSD) of individual fluorescence measurements taken from

nine separate areas within each well correlated strongly with the loading patterns (Figure 3C, Figure S2). For all tested MNP doses, the optimized protocol resulted in RSD consistently below 15%, compared to several-fold greater RSD values of 126±8% and 47±6% determined for EC treated with the lowest and highest MNP doses (1 and 10 μg per well, respectively) using the non-uniform process, suggesting that RSD of a series of measurement taken across the area of a well can provide a practical quantitative metric of the MNP distribution uniformity. Unlike uniformly loaded cells fully retaining viability and metabolic activity at all tested particle doses (viability loss <3% at 10 μg MNP per well, Figure 3D), non-uniformly loaded EC revealed a significant loss of viability increasing rapidly with MNP amount (p<0.001) and reaching 30±12% at the highest dose of 10 μg MNP per well. Collectively, the results of these studies point to several important observations. First, using stably fluorescently labeled MNP we showed that cell loading processes can exert dramatically different effects on the viability status of functionalized cells as a result of variations in MNP uptake uniformity. Second, our findings suggest that, in combination with fluorescent microscopy as an approach for detecting unbalanced MNP distribution at the microscopic scale, fluorimetric measurements of internalized MNP conducted over a cell-covered area in the well-scan mode provide a simple and sensitive method for obtaining accurate quantitative estimates of cell functionalization uniformity. Specifically, the RSD of the MNP-associated fluorescent signal sampled from a number of different regions within a well provides a quantitative measure accurately reflecting (in)homogeneity of MNP distribution over a broad range of MNP doses. Thus, cell loading protocol optimization may include the establishment of threshold RSD values corresponding to a maximal acceptable variability in MNP distribution, helping to reduce toxicity and improve quality of magnetically targetable cell preparations.

The effect of cell functionalization uniformity on magnetic capture was studied as a function of MNP loading and exposure duration in another set of experiments using the inverted-plate method (Figure 4, Figure S3). The magnetic capture efficiencies of EC loaded with MNP using the two protocols were found to be markedly dissimilar, both in terms of captured cell fractions and initial cell depletion rates (Figure 4A). For the optimized protocol, the proportion of magnetically captured EC was directly dependent on MNP dose and exposure duration, with more than 50% of uniformly loaded cells captured within 5 min at all tested MNP doses above 0.5 μg per well (Figure S3A). Furthermore, a 1 min-long magnetic exposure was already sufficient to capture 49.5±9.8% of EC functionalized with 10 μg MNP per well (Figure 4B). The high capture rates approaching or exceeding 50% and the stable cell anchorage in the presence of a competing force after a short exposure (on the order of 1–5 min) observed in the present study may be of particular relevance to the clinical settings of magnetically targeted cell delivery, where the exposure duration may be a significant limiting factor. In comparison, magnetic capture of EC loaded non-uniformly exhibited a bell-shaped dependence on MNP dose at all tested exposure durations (Figure S3B), with the highest cell depletion rates observed at 1 μg MNP per well and rapidly declining toward 10 μg/well (Figure 4B). Reaching the maximal fractional capture of ca. 50% required prolonging the magnetic exposure to 30 min, whereas the proportion of EC captured after 5 min was consistently below 20% for all MNP doses (Figure S3B). This difference in the cell capture patterns is a result of the dual selection built into the assay design: only cells

exhibiting a combination of magnetic responsiveness sufficient to drive their motion against gravity with unaltered viability and substrate binding capacity will demonstrate capture and stable anchorage. Thus, the bell-shaped pattern of cell depletion and the generally poor capture efficiency of EC loaded with MNP using the protocol simulating non-uniform distribution of the MNP payload is attributed to the presence of underloaded (insufficiently magnetically responsive) and overloaded (non-viable) cells, whose proportions additionally increase toward the lower and higher tested MNP doses, respectively.

The profound effect of loading uniformity on magnetic guidance capacity demonstrated using the inverted-plate assay was reevaluated using magnetophoretic cell mobility/capture measurements. Magnetic capture was monitored and analyzed for each cell loading protocol as a function of MNP dose. Remarkably, capture kinetics measured in parallel using the distinct fluorescent signals of MNP (red: $\lambda_{ex}/\lambda_{em}$ = 540 nm/575 nm) and a lipophilic cyanine dye used to label EC (green: $\lambda_{ex}/\lambda_{em}$ = 485 nm/535 nm) were near-identical for cells functionalized using the optimized protocol (Figure S4A), consistent with previously shown high loading uniformity (Figure 3A–B and Figure S2). A direct comparison between the magnetic capture profiles of cells loaded using the two protocols closely reiterated the trends observed with the inverted-plate assay: while cell capture was consistently incomplete within the time frame of the experiment (0–30 min) likely due to a small fraction of EC remaining outside the rapid capture zone,[21] cells loaded with high uniformity using the optimized protocol exhibited rapid capture (over 50% EC loaded at 5 and 1 μg/well were depleted within 10 sec and 4 min, respectively, Figure 5AμB). Furthermore, magnetic capture of EC functionalized using this protocol with MNP at doses ≥5 μg/well was 77±2% complete already after 30 sec. In contrast, the maximal capture rates (measured at 30 min) remained on average below 50% for EC loaded with all doses of MNP using the protocol modeling non-uniform payload distribution. The markedly more effective capture of uniformly functionalized cells within a time frame practically relevant to the clinical settings of magnetically guided delivery is confirmed by detailed analysis of the early time points (0–3 min, Figure 5B), as well as the initial cell capture rates (Figure 5C). Whereas magnetic depletion of uniformly loaded cells measured over the first 60 sec occurred with high rates, which were also directly dependent on the MNP dose (0.46±0.10%, 1.12±0.09%, and 1.23±0.04% per sec for 1, 5 and 10 μg MNP per well, respectively), the initial capture of EC loaded using the alternative protocol exhibited significantly slower kinetics repeating the characteristic bell-shaped dependence on the MNP dose (0.22±0.07, 0.36±0.09, and 0.16±0.18% per sec for 1, 5, and 10 μg MNP per well, respectively). Thus, the markedly dissimilar performances of EC loaded using two protocols become most evident at larger MNP doses, with almost an order of magnitude greater initial capture rates of EC uniformly loaded with MNP at a dose of 10 μg/well. The strong interdependence of the loading protocol and the effect of the MNP dose was confirmed by statistical analysis (p<0.001, two-way ANOVA), with significant differences between the two loading procedures demonstrated at each tested dose of MNP (p<0.02).

The results of inverted-plate experiments and magnetophoretic EC capture studies together demonstrate that cell functionalization uniformity is essential for achieving efficient magnetic guidance on a clinically relevant time scale, as well as for minimizing the fraction of cells prone to dissemination to non-target sites. Underloaded and overloaded cells present

in non-uniform preparations (Figure 1) lack either the magnetic responsiveness or capacity for stable anchorage required for guided, site-specific delivery and retention. Thus, their presence is likely to reduce the overall therapeutic efficacy of a treatment, while at the same time considerably increasing the risk of serious adverse effects, including formation of emboli, impaired tissue function due to off-target paracrine effects or procoagulant activity leading to thrombotic events.[28–29] While, in contrast to the inverted-plate assay, magnetophoretic cell mobility/depletion studies do not address viability and substrate attachment capacity of the captured cells, the results of these two sets of experiments are in agreement, pointing to similar trends with regard to the individual effects and interaction between cell loading uniformity and MNP dose. Remarkably, these trends were shown to be present both on an extended time scale up to 30 min, as well as at early time points as evident from the comparative analysis of initial cell depletion kinetics (Figure 5C). To be of practical relevance and utility for site-specific cell delivery, a cell functionalization process should allow rapid and effective magnetic guidance of MNP-loaded cells in the presence of competing forces to allow near-quantitative cell capture and stable homing to the delivery site over a short period of time, on the scale of several minutes. Loading uniformity appears to be the key characteristic of a cell preparation determining both the overall efficiency and the kinetic pattern of magnetic cell capture.

Our findings show that the robustness of cell products can be markedly increased by using a cell functionalization protocol optimized for payload distribution uniformity: smaller amounts of MNP can be applied without significantly compromising the rates of magnetic cell capture/retention. This may be of particularly importance when MNP are formulated with small-molecule therapeutics or gene delivery vectors as modifiers of the cell biological activity,[21, 30] which in turn may require precise control over the dose of the particles in order to avoid untoward effects on the delivered cells or cellular components of the tissue near the site of their homing. At the same time, uniform distribution of the MNP payload makes possible accelerating the capture process and maximizing the fractional capture rates by enabling safe use of larger doses of MNP formulations with enhanced biocompatibility, such as that in the present study shown to have no significant cell toxic effects up to 160 pg iron oxide per cell.[21] The robustness of the uniformly loaded cell preparation observed over a broad range of MNP doses is in contrast to the bell-shaped magnetic capture pattern characterizing non-uniformly loaded cells (Figures 4 and 5), with inferior fractional capture rates at all tested time points and with all MNP doses. Based on our results, cell functionalization protocols optimized for uniformity offer greater flexibility with regard to loading conditions and MNP dose, which is advantageous for adjusting the cell production process for a given therapeutic application. This robustness is essential for maintaining the balance between adequate magnetic responsiveness and acceptable biological function of the cell product for consistent efficiency and safety of its clinical use. Furthermore, as cryopreservation is an important part of the cell preparation process (addressed by our group in a previous study[6]), the uniform distribution of the MNP payload is likely to reduce the cytoskeleton destabilization[20, 31] and increase the ability of the cells to withstand the stress associated with freezing, making possible rapid recovery of normal morphology and proliferation rates after storage, whereas non-uniform loading resulting in a significant

proportion of overloaded cells can increase their vulnerability to the injury associated with the cell freezing process.

Conclusions

Magnetically guided delivery has shown promise as a strategy for enhancing target specificity, efficacy, and safety of cell therapies for a broad spectrum of diseases currently lacking effective treatment options.[32] The successful translation of magnetic cell guidance to the clinic requires elucidating key factors governing cell functionalization and reliably determining the effect of these process variables on the magnetic properties and biological function of the cell product. To address the need for a single-platform approach providing unbiased results and accurately reflecting both adequacy and variability of the relevant cell characteristics within a preparation, we developed an inverted-plate assay and applied it to comparatively analyze the performance of two cell loading protocols providing distinct patterns of MNP uptake, varying in degrees of the particle distribution uniformity across the cells. The profound difference between the two cell loading protocols with markedly faster magnetic capture kinetics occurring on a clinically relevant time scale, followed by stable anchorage and rapid expansion of uniformly functionalized cells, was demonstrated by the inverted-plate assay and confirmed by well-scan fluorimetric measurements and magnetophoretic mobility analysis, emphasizing the importance of thoroughly optimizing the cell preparation process with regard to uniformity. Achieving well-balanced MNP payload distribution is key to robust production of magnetically targetable cells with fully preserved viability, substrate binding capacity, and regeneration potential. The results of our study and the new single-platform assay developed as a tool for optimizing the performance of cell loading protocols and magnetically functionalized cells are expected to inform their evaluation in experimental disease models and subsequently facilitate translation of targeted cell therapeutics to the clinic.

Methods

Formulation and characterization of MNP

Particle-forming polymer covalently labeled with $BODIPY_{558/568}$ (5.7 μmol per gram) was synthesized from poly(D,L-lactide) with M_n of 50 kDa (Lakeshore Biomaterials, Birmingham, AL) as previously described[25]. Uniformly sized, polylactide (PLA)-based magnetic nanoparticles were formulated using a modification of the emulsification-solvent evaporation method.[21] The composite design of the particles obtained using this formulation approach, with multiple individual small-sized magnetite nanocrystals incorporated in the rigid particle matrix, is key to their superparamagnetic behavior and negligible magnetic remanence (less than 1% of the respective saturation value).[21, 33] In brief, 2.5 mL of an ethanolic solution containing 170 mg ferric chloride and 62.5 mg ferrous chloride tetrahydrate was mixed with an equal volume of sodium hydroxide dissolved in deionized water (0.5 M). The precipitate was matured at 90 °C for 1 min, then cooled on ice. The formed magnetite was separated using a magnet and dispersed under constant mixing over 5 min at 90 °C in 2 mL of an ethanolic solution containing 200 mg oleic acid. The excess of oleic acid was removed *via* phase separation with 4 mL deionized water and decantation.

Oleic acid-coated magnetite was washed with ethanol and dispersed in 4 mL of chloroform. An equal volume of a chloroformic solution containing $BODIPY_{558/568}$-labeled and plain PLA (80 mg and 120 mg, respectively) was added to the magnetite suspension to form an organic phase. The organic phase was emulsified with 10 mL of aqueous bovine serum albumin (2%, w/v) by sonication on ice, followed by the removal of the organic solvent under reduced pressure using a rotary evaporator. Formed MNP were washed twice with deionized water using magnetic decantation, then resuspended in 6 mL of aqueous trehalose solution (10%, w/v), filtered through a sterile 5.0-μm polyvinylidene difluoride membrane (EMD Millipore; Billerica, MA), and lyophilized. Lyophilized MNP were stored at −20 °C and reconstituted in deionized water to 22 mg/mL (Barnstead Nanopure; Thermo Scientific, Dubuque, IA, USA) before use.

Dynamic light scattering (90 Plus Particle Size Analyzer, Brookhaven Instruments; Holtsville, NY) was used to characterize MNP size. Magnetite content of the MNP was determined spectrophotometrically against a standard curve (λ = 335) after digesting MNP in 1 M sodium hydroxide for 30 min, then dissolving the iron oxide precipitate in 1 M hydrochloric acid at 90 °C for 5 min.

EC functionalization with MNP and characterization of loading uniformity

Bovine aortic EC (BAEC) were cultured in DMEM supplemented with 10% FBS at 37 °C in a humidified atmosphere of 5% CO_2−95% air. One day prior to functionalization, BAEC were seeded on a 96-well plate at 12×10^3 cells/well and allowed to reach confluency overnight. On the next day, BAEC were washed with culture medium prior to loading with MNP, using either the optimized (uniform) procedure or a modified protocol modeling uneven MNP payload distribution as described below.

Uniform EC loading using an optimized procedure.—BAEC uniformly loaded with MNP were produced using a procedure based on magnetically enhanced endocytosis, optimized and applied previously to functionalize EC for *in vitro* studies and magnetically guided cell delivery in an animal model of arterial restenosis[6, 21, 25]. Briefly, MNP were diluted to indicated amounts with culture medium and added to BAEC at 100 μL/well. To promote concurrent sedimentation and endocytosis of MNP, the plate was positioned on a magnetic separator with an average field gradient of 32.5 T/m (LifeSep™ 96 F, Dexter Magnetic Technologies; Fremont, CA) and incubated at 37°C for 24 hr for complete internalization of the MNP payload.[21]

Non-uniform EC loading using a (simulated) procedure designed to model uneven MNP distribution.—A modified procedure was developed to model uneven distribution of MNP across cells within a well. Prior to loading, plated BAEC were incubated at 4 °C for 30 min to temporarily inhibit endocytosis. Indicated amounts of MNP were diluted in chilled culture medium to a volume of 1 μL. While the plate was on the magnetic separator, the concentrated suspension of MNP was added to the rightmost region of the culture medium-containing wells, in the immediate vicinity of the seeded cells. The plate with the magnetic separator was returned to 4 °C for an additional 30 min to

concentrate the MNP on the cell surface while inhibiting their internalization. Afterwards, the plate was transferred together with the magnetic separator to a 37°C incubator for 24 hr.

The spatial distribution of MNP after completion of cell loading with either procedure was characterized fluorimetrically ($\lambda_{ex}/\lambda_{em}$ = 540 nm/575 nm) using the scan-mode settings at nine regions equally spaced throughout the well (SpectraMax Gemini EM, Molecular Devices; Sunnyvale, CA). These values were used to calculate the averages and relative standard deviations (RSD) of the MNP payload distribution. Cell viability was evaluated using the resazurin (Alamar Blue) assay.[34] To selectively determine the fluorescent signal of the dye reduced to resorufin by aerobic respiration of the metabolically active cells, the supernatant was transferred into empty wells immediately before the measurement and its emission was read at $\lambda_{ex}/\lambda_{em}$ = 540 nm/575 nm.

Evaluation of EC functionality using the inverted-plate assay

The magnetic guidance capacity of EC in the presence of a challenging (gravitational) force, anchorage and proliferation were evaluated longitudinally as a function of MNP dose and cell loading protocol using the inverted-plate assay. MNP-loaded BAEC were washed, trypsinized, suspended in culture medium and applied in quadruplicates at 270 μL per well to the wells of a 96-well plate. The plate was overturned gently with the suspensions retained within the wells of the plate. The plate was incubated at 37 °C for 1, 5, 15, and 30 min with a magnetic separator (average field strength = 32.5 T/m) placed atop the plate to apply a high-gradient magnetic field directionally opposite to that of the gravitational force. After incubation, the supernatants containing unattached cells were transferred into fresh wells. Substrate-adherent and unattached cells were enumerated both by manual counting and the Alamar Blue assay.[34] The proliferation rate of captured BAEC was determined by measuring cell numbers at 24-hr intervals, using non-functionalized cells seeded at an equal density as a reference.

Magnetic cell capture studies using depletion-based magnetophoresis

The characterization of magnetic responsiveness using the inverted-plate assay was cross-validated using a depletion-based magnetophoresis assay adapted from a previously described procedure.[35] MNP-loaded BAEC were first stained with the fluorescent membrane probe, 3,3-dioctadecyloxacarbocyanine perchlorate (ChemCruz; Dallas, TX), diluted to 10 μM in culture medium and applied for 3 hr at 37 °C. Fluorescently labeled cells were collected through trypsinization, washed *via* centrifugation in DPBS supplemented with 10% FBS, then resuspended in DPBS supplemented with 1% FBS. Cell suspensions were applied to a 48-well plate at 1 mL per well, and their fluorescent signals were measured in 10-sec intervals at 37°C at $\lambda_{ex}/\lambda_{em}$ = 485 nm/535 nm (SpectraMax Gemini EM, Molecular Devices; Sunnyvale, CA). The magnetically driven cell capture was accomplished using two mutually attracting neodymiumiron-boron magnets (L×H×D: 18 mm×12 mm×6 mm) placed around the well. The field strength was measured to be 0.35 T and 0.24 T at the surface and the center of the well, respectively (Model 410 Gaussmeter, Lakeshore; Westerville, OH). Fractional EC capture values and initial capture rates were derived from changes in normalized fluorescence intensities of cell suspensions (I_t normalized against I_0, or I_t/I_0) over time.

Statistical Analysis

Experimental data are expressed as mean ± standard deviation. Cell proliferation kinetics were analyzed by linear regression. Results were evaluated using one-way or two-way analysis of variance (ANOVA) with the Bonferroni correction for multiple comparisons where appropriate. Differences were termed significant at $p<0.05$.

Supplementary Material

Refer to Web version on PubMed Central for supplementary material.

Acknowledgements

This research was supported by U.S. National Heart, Lung, and Blood Institute grants T32-HL007915 (MRB), R01-HL111118 and R21-HL131016 (MC), a grant from The W.W. Smith Charitable Trust, and The Children's Hospital of Philadelphia Research Funds including the William J. Rashkind Endowment, Erin's Fund, and The Kibel Foundation (RJL).

References

1. Buzhor E; Leshansky L; Blumenthal J; Barash H; Warshawsky D; Mazor Y; Shtrichman R, Cell-Based Therapy Approaches: The Hope for Incurable Diseases. Regen Med 2014, 9, 649–72. [PubMed: 25372080]
2. Chen CH; Sereti KI; Wu BM; Ardehali R, Translational Aspects of Cardiac Cell Therapy. J Cell Mol Med 2015, 19, 1757–72. [PubMed: 26119413]
3. Holloway JL, Fighting for Their Lives: A Strategy for Improved Cell Transplantation Survival. Sci Transl Med 2018, 10, eaar7536.
4. Li L; Chen X; Wang WE; Zeng C, How to Improve the Survival of Transplanted Mesenchymal Stem Cell in Ischemic Heart? Stem Cells Int 2016, 2016, 9682757. [PubMed: 26681958]
5. Sarkar D; Spencer JA; Phillips JA; Zhao W; Schafer S; Spelke DP; Mortensen LJ; Ruiz JP; Vemula PK; Sridharan R; Kumar S; Karnik R; Lin CP; Karp JM, Engineered Cell Homing. Blood 2011, 118, e184–91. [PubMed: 22034631]
6. Adamo RF; Fishbein I; Zhang K; Wen J; Levy RJ; Alferiev IS; Chorny M, Magnetically Enhanced Cell Delivery for Accelerating Recovery of the Endothelium in Injured Arteries. J Control Release 2016, 222, 169–75. [PubMed: 26704936]
7. Fagg WS; Liu N; Yang MJ; Cheng K; Chung E; Kim JS; Wu G; Fair J, Magnetic Targeting of Stem Cell Derivatives Enhances Hepatic Engraftment into Structurally Normal Liver. Cell Transplant 2017, 26, 1868–1877. [PubMed: 29390880]
8. Mahmoud EE; Kamei G; Harada Y; Shimizu R; Kamei N; Adachi N; Misk NA; Ochi M, Cell Magnetic Targeting System for Repair of Severe Chronic Osteochondral Defect in a Rabbit Model. Cell Transplant 2016, 25, 1073–83. [PubMed: 26419946]
9. Muthana M; Kennerley AJ; Hughes R; Fagnano E; Richardson J; Paul M; Murdoch C; Wright F; Payne C; Lythgoe MF; Farrow N; Dobson J; Conner J; Wild JM; Lewis C, Directing Cell Therapy to Anatomic Target Sites in Vivo with Magnetic Resonance Targeting. Nat Commun 2015, 6, 8009. [PubMed: 26284300]
10. Orynbayeva Z; Sensenig R; Polyak B, Metabolic and Structural Integrity of Magnetic Nanoparticle-Loaded Primary Endothelial Cells for Targeted Cell Therapy. Nanomedicine (Lond) 2015, 10, 1555–68. [PubMed: 26008193]
11. Polyak B; Medved M; Lazareva N; Steele L; Patel T; Rai A; Rotenberg MY; Wasko K; Kohut AR; Sensenig R; Friedman G, Magnetic Nanoparticle-Mediated Targeting of Cell Therapy Reduces in-Stent Stenosis in Injured Arteries. ACS Nano 2016, 10, 9559–9569. [PubMed: 27622988]
12. Vosen S; Rieck S; Heidsieck A; Mykhaylyk O; Zimmermann K; Bloch W; Eberbeck D; Plank C; Gleich B; Pfeifer A; Fleischmann BK; Wenzel D, Vascular Repair by Circumferential Cell

Therapy Using Magnetic Nanoparticles and Tailored Magnets. ACS Nano 2016, 10, 369–76. [PubMed: 26736067]

13. Zohra FT; Medved M; Lazareva N; Polyak B, Functional Behavior and Gene Expression of Magnetic Nanoparticle-Loaded Primary Endothelial Cells for Targeting Vascular Stents. Nanomedicine (Lond) 2015, 10, 1391–406. [PubMed: 25996117]
14. Huang Z; Shen Y; Pei N; Sun A; Xu J; Song Y; Huang G; Sun X; Zhang S; Qin Q; Zhu H; Yang S; Yang X; Zou Y; Qian J; Ge J, The Effect of Nonuniform Magnetic Targeting of Intracoronary-Delivering Mesenchymal Stem Cells on Coronary Embolisation. Biomaterials 2013, 34, 9905–16. [PubMed: 24055521]
15. Tefft BJ; Uthamaraj S; Harburn JJ; Hlinomaz O; Lerman A; Dragomir-Daescu D; Sandhu GS, Magnetizable Stent-Grafts Enable Endothelial Cell Capture. J Magn Magn Mater 2017, 427, 100–104. [PubMed: 28286359]
16. Lu Y-C; Chang F-Y; Tu S-J; Chen J-P; Ma Y-H, Cellular Uptake of Magnetite Nanoparticles Enhanced by Ndfeb Magnets in Staggered Arrangement. Journal of Magnetism and Magnetic Materials 2017, 427, 71–80.
17. Riegler J; Liew A; Hynes SO; Ortega D; O'Brien T; Day RM; Richards T; Sharif F; Pankhurst QA; Lythgoe MF, Superparamagnetic Iron Oxide Nanoparticle Targeting of Mscs in Vascular Injury. Biomaterials 2013, 34, 1987–94. [PubMed: 23237516]
18. Jing Y; Mal N; Williams PS; Mayorga M; Penn MS; Chalmers JJ; Zborowski M, Quantitative Intracellular Magnetic Nanoparticle Uptake Measured by Live Cell Magnetophoresis. FASEB J 2008, 22, 4239–47. [PubMed: 18725459]
19. Kyrtatos PG; Lehtolainen P; Junemann-Ramirez M; Garcia-Prieto A; Price AN; Martin JF; Gadian DG; Pankhurst QA; Lythgoe MF, Magnetic Tagging Increases Delivery of Circulating Progenitors in Vascular Injury. JACC Cardiovasc Interv 2009, 2, 794–802. [PubMed: 19695550]
20. Soenen SJ; Himmelreich U; Nuytten N; De Cuyper M, Cytotoxic Effects of Iron Oxide Nanoparticles and Implications for Safety in Cell Labelling. Biomaterials 2011, 32, 195–205. [PubMed: 20863560]
21. Chorny M; Alferiev IS; Fishbein I; Tengood JE; Folchman-Wagner Z; Forbes SP; Levy RJ, Formulation and in Vitro Characterization of Composite Biodegradable Magnetic Nanoparticles for Magnetically Guided Cell Delivery. Pharm Res 2012, 29, 1232–41. [PubMed: 22274555]
22. Chorny M; Fishbein I; Adamo RF; Forbes SP; Folchman-Wagner Z; Alferiev IS, Magnetically Targeted Delivery of Therapeutic Agents to Injured Blood Vessels for Prevention of in-Stent Stenosis. Methodist DeBakey Cardiovasc J 2012, 8, 23–7. [PubMed: 22891107]
23. O'Brien J; Wilson I; Orton T; Pognan F, Investigation of the Alamar Blue (Resazurin) Fluorescent Dye for the Assessment of Mammalian Cell Cytotoxicity. Eur J Biochem 2000, 267, 5421–6. [PubMed: 10951200]
24. Huang L; Han G, Near Infrared Boron Dipyrromethene Nanoparticles for Optotheranostics. Small Methods 2018, 2, 1700370. [PubMed: 31872045]
25. Tengood JE; Alferiev IS; Zhang K; Fishbein I; Levy RJ; Chorny M, Real-Time Analysis of Composite Magnetic Nanoparticle Disassembly in Vascular Cells and Biomimetic Media. Proc Natl Acad Sci U S A 2014, 111, 4245–4250. [PubMed: 24591603]
26. Delcroix GJ; Jacquart M; Lemaire L; Sindji L; Franconi F; Le Jeune JJ; Montero-Menei CN, Mesenchymal and Neural Stem Cells Labeled with Hedp-Coated Spio Nanoparticles: In Vitro Characterization and Migration Potential in Rat Brain. Brain Res 2009, 1255, 18–31. [PubMed: 19103182]
27. Sharkey J; Starkey Lewis PJ; Barrow M; Alwahsh SM; Noble J; Livingstone E; Lennen RJ; Jansen MA; Carrion JG; Liptrott N; Forbes S; Adams DJ; Chadwick AE; Forbes SJ; Murray P; Rosseinsky MJ; Goldring CE; Park BK, Functionalized Superparamagnetic Iron Oxide Nanoparticles Provide Highly Efficient Iron-Labeling in Macrophages for Magnetic Resonance-Based Detection in Vivo. Cytotherapy 2017, 19, 555–569. [PubMed: 28214127]
28. Caplan H; Olson SD; Kumar A; George M; Prabhakara KS; Wenzel P; Bedi S; Toledano-Furman NE; Triolo F; Kamhieh-Milz J; Moll G; Cox CS Jr., Mesenchymal Stromal Cell Therapeutic Delivery: Translational Challenges to Clinical Application. Front Immunol 2019, 10, 1645. [PubMed: 31417542]

29. Korhonen M; Jolkkonen J, Intravascular Cell Therapy in Stroke Patients: Where the Cells Go and What They Do. Regen Med 2013, 8, 93–5. [PubMed: 23477388]

30. Battig MR; Fishbein I; Levy RJ; Alferiev IS; Guerrero D; Chorny M, Optimizing Endothelial Cell Functionalization for Cell Therapy of Vascular Proliferative Disease Using a Direct Contact Co-Culture System. Drug Deliv Transl Res 2018, 8, 954–963. [PubMed: 28755158]

31. Soenen SJ; Nuytten N; De Meyer SF; De Smedt SC; De Cuyper M, High Intracellular Iron Oxide Nanoparticle Concentrations Affect Cellular Cytoskeleton and Focal Adhesion Kinase-Mediated Signaling. Small 2010, 6, 832–42. [PubMed: 20213651]

32. Connell JJ; Patrick PS; Yu Y; Lythgoe MF; Kalber TL, Advanced Cell Therapies: Targeting, Tracking and Actuation of Cells with Magnetic Particles. Regen Med 2015, 10, 757–72. [PubMed: 26390317]

33. Chorny M; Fishbein I; Yellen BB; Alferiev IS; Bakay M; Ganta S; Adamo R; Amiji M; Friedman G; Levy RJ, Targeting Stents with Local Delivery of Paclitaxel-Loaded Magnetic Nanoparticles Using Uniform Fields. Proc Natl Acad Sci U S A 2010, 107, 8346–51. [PubMed: 20404175]

34. O'Brien J; Wilson I; Orton T; Pognan F, Investigation of the Alamar Blue (Resazurin) Fluorescent Dye for the Assessment of Mammalian Cell Cytotoxicity. Eur. J. Biochem. 2000, 267, 5421–5426. [PubMed: 10951200]

35. Grzeskowiak BF; Sanchez-Antequera Y; Hammerschmid E; Doblinger M; Eberbeck D; Wozniak A; Slomski R; Plank C; Mykhaylyk O, Nanomagnetic Activation as a Way to Control the Efficacy of Nucleic Acid Delivery. Pharm. Res. 2015, 32, 103–121. [PubMed: 25033763]

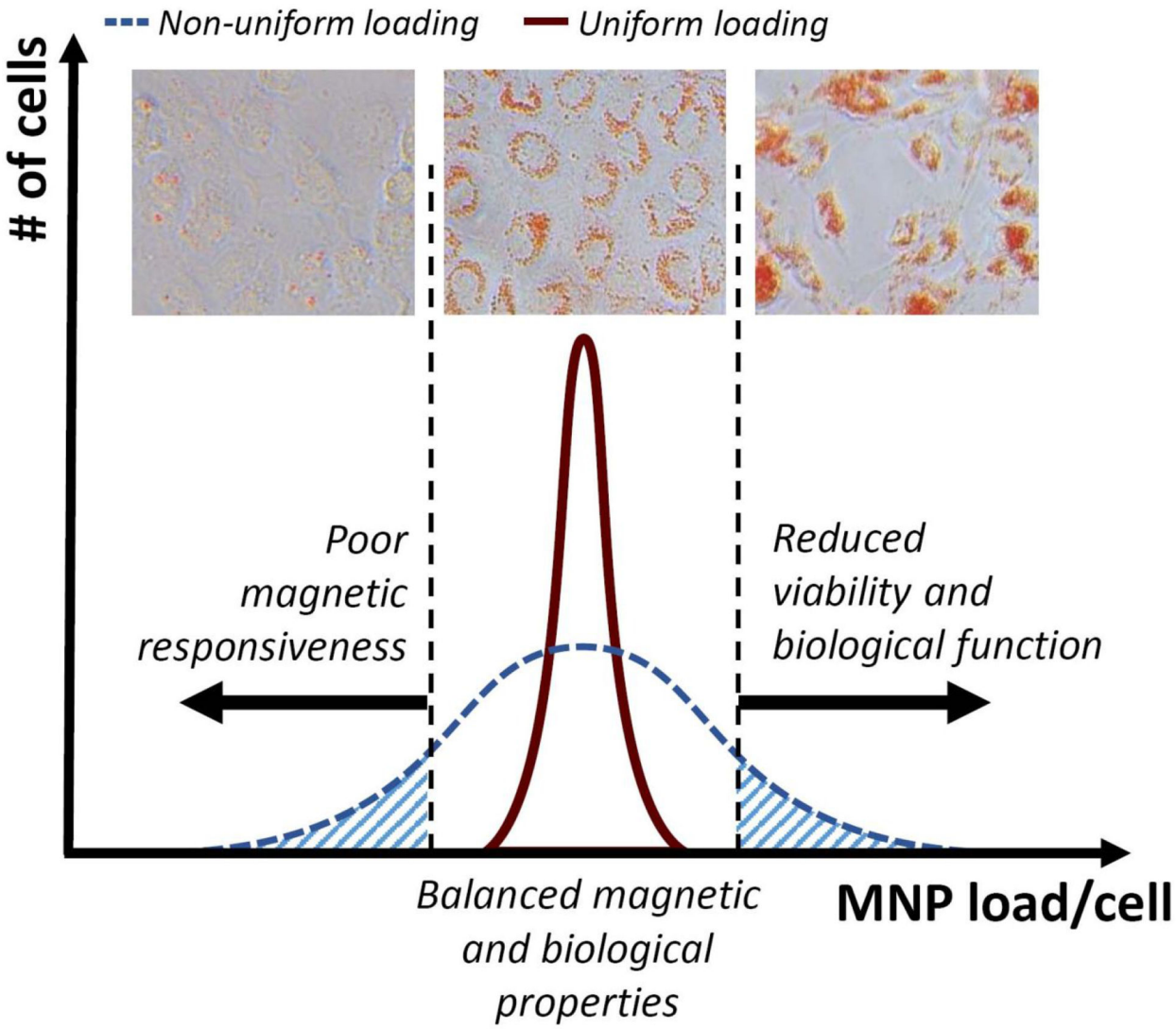

Figure 1.

Scheme illustrating the effect of the uniformity of cell functionalization with MNP for magnetically guided delivery. The pattern of magnetically driven MNP uptake determines both the magnetic guidance capacity and the ability of cells to stably home and expand at the target site.

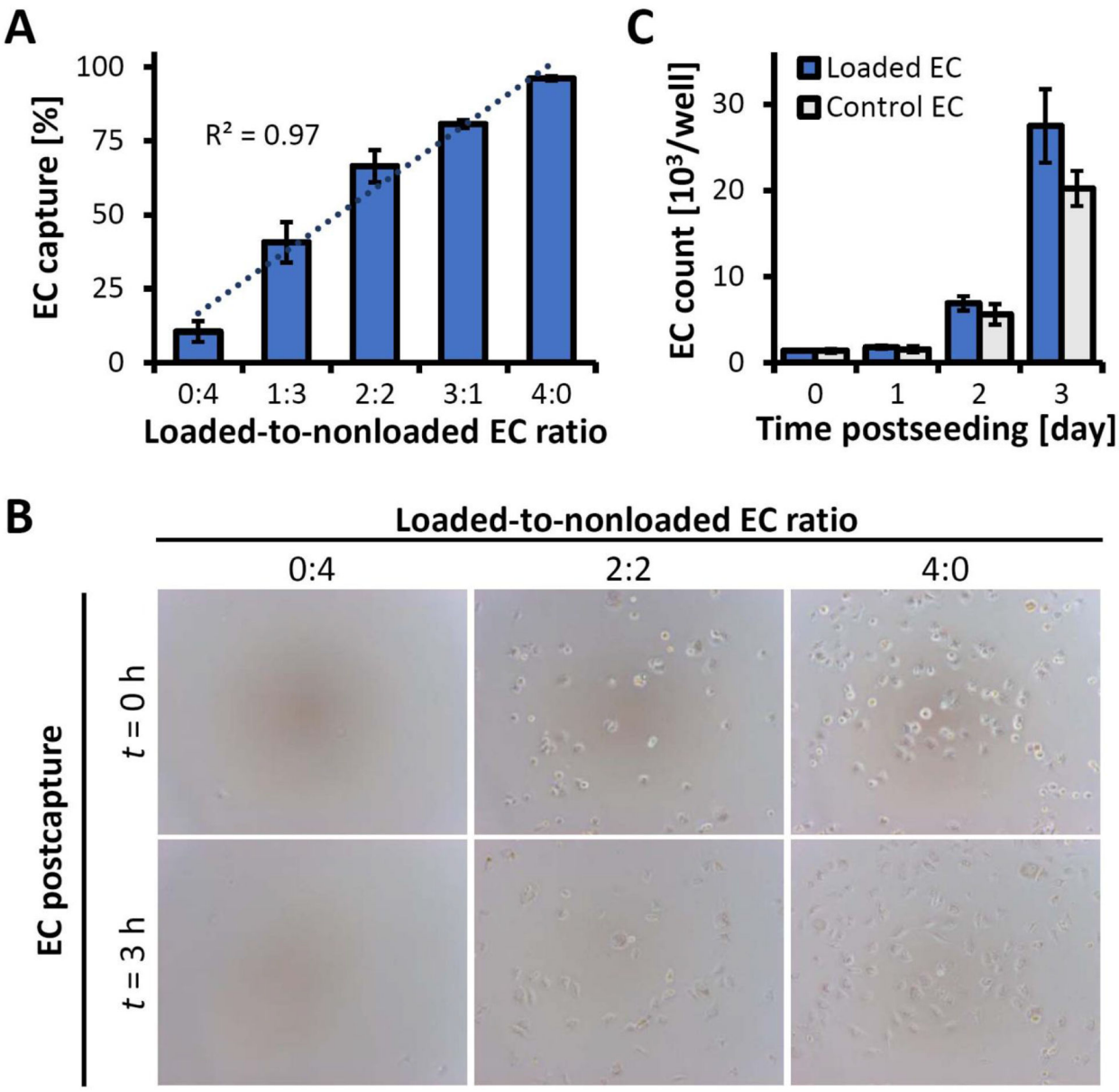

Figure 2.

Characterization of magnetic responsiveness, substrate binding stability and EC growth using the inverted-plate assay. (**A**) EC capture from binary suspensions of MNP-loaded and non-loaded EC showing selective and quantitative separation of magnetically responsive cells at all tested ratios. (**B**) Representative micrographs of EC captured from binary mixtures immediately following capture (t = 0 hr) and 3 hr post-capture, showing magnetically driven substrate attachment and stable anchorage (magnification ×100). (**C**) The number of magnetically captured, functionalized EC (“Loaded EC”) 0–3 days post-seeding, shown in comparison to non-functionalized control cells seeded at the same initial density (“Control EC”). Statistical analysis shows no significant difference in the proliferation kinetics (p=0.4).

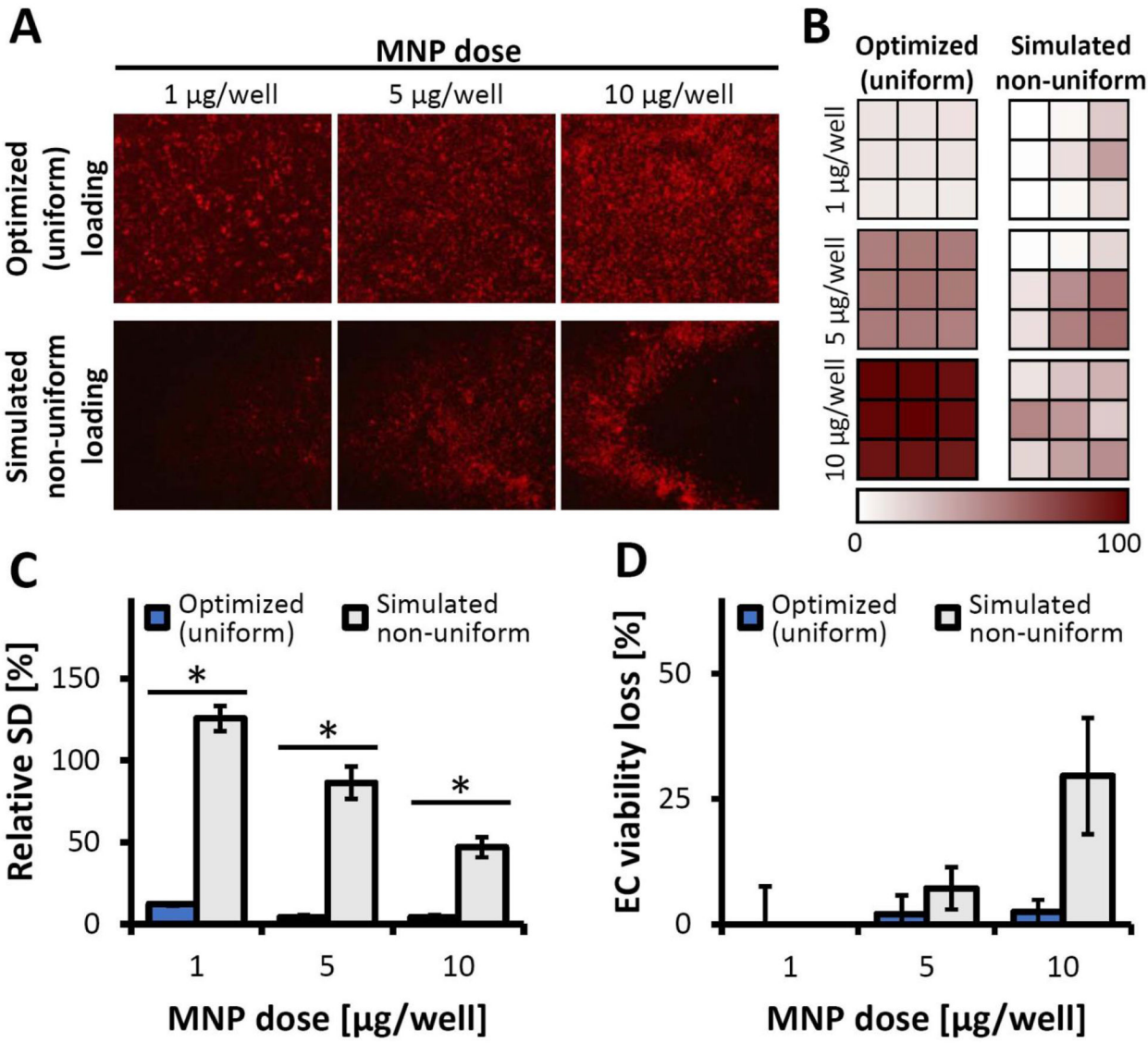

Figure 3.

The effect of cell loading protocol on uniformity of MNP distribution. (**A**) Representative fluoromicrographs showing MNP distribution within a well following cell functionalization using optimized *vs.* simulated non-uniform loading conditions (magnification: ×40). (**B**) MNP distributions presented as well-scan fluorescence intensity plots from signals sampled across nine areas equally spaced throughout the well. A gradient color scale is used to express local fluorescence intensities as a percentage of the maximum fluorescent signal. (**C**) Relative standard deviations (RSD) of the well-scan fluorescence intensities calculated as a measure of uptake uniformity. (**D**) The comparative viabilities of EC loaded with MNP using two protocols, assessed using the Alamar Blue assay against non-treated EC as a reference. Both loading procedure, MNP dose, and their interaction had significant effects on EC viability per the results of two-way ANOVA analysis ($p < 0.001$ for each effect). An * denotes a statistically significant difference between the optimized (uniform) loading and the simulated, non-uniform loading of EC at the specified dose of MNP.

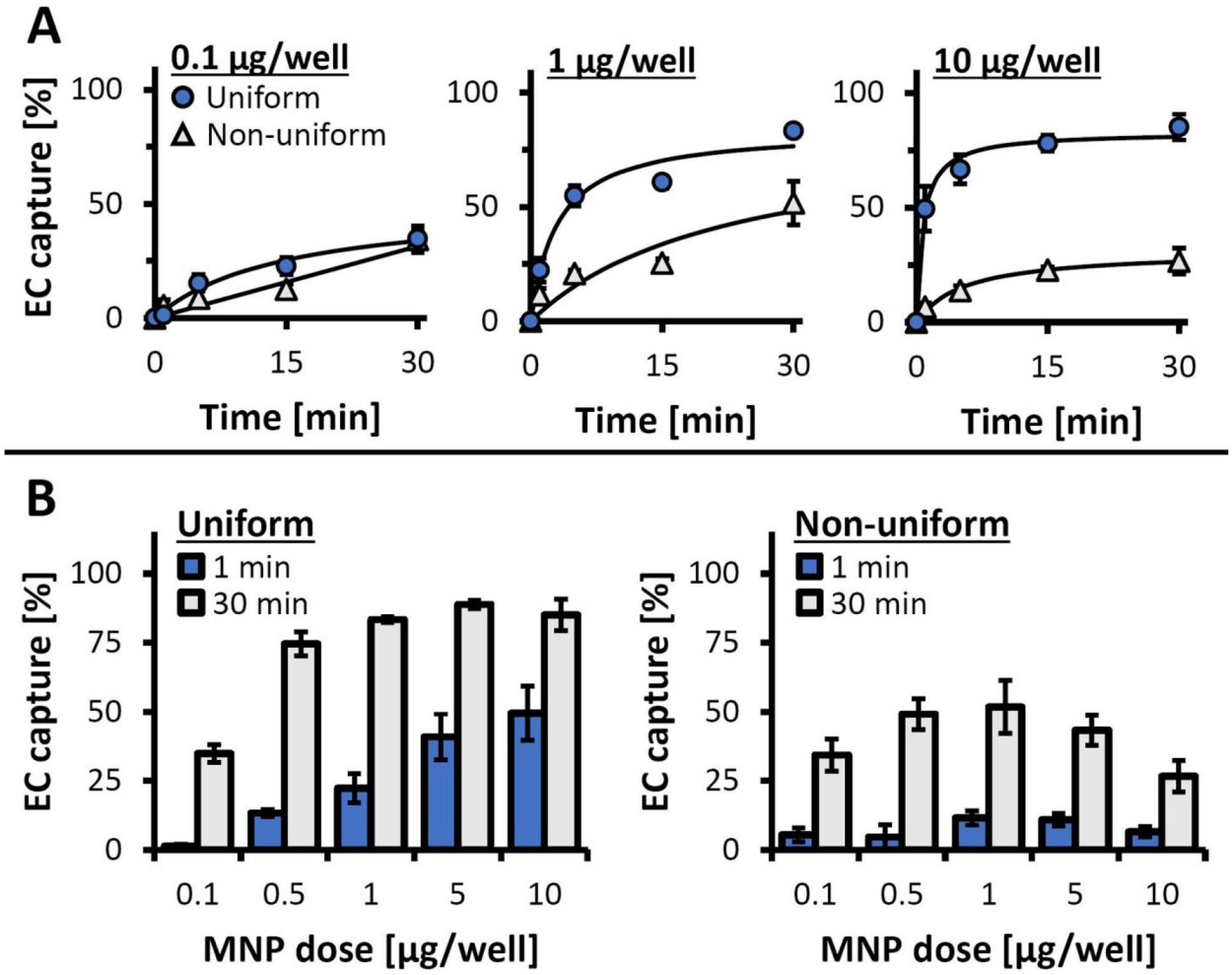

Figure 4.

Magnetic EC capture/anchorage measured longitudinally using the inverted-plate assay as a function of loading protocol and MNP dose. (**A**) The time courses of EC capture are shown for EC loaded using 0.1, 1, and 10 μg MNP/well with the optimized (uniform) and the simulated, non-uniform loading procedures. EC captured by exposure to the high-gradient magnetic field over different time periods (1, 5, 15, and 30 min) were quantified using the Alamar Blue assay. Data are presented as a fraction of the total cell number ($n = 4$). (**B**) Detailed analysis of EC capture/anchorage after 1 and 30 min of magnetic exposure for EC loaded with 0.1–10 μg MNP/well using the optimized (uniform) and the simulated, non-uniform loading procedures.

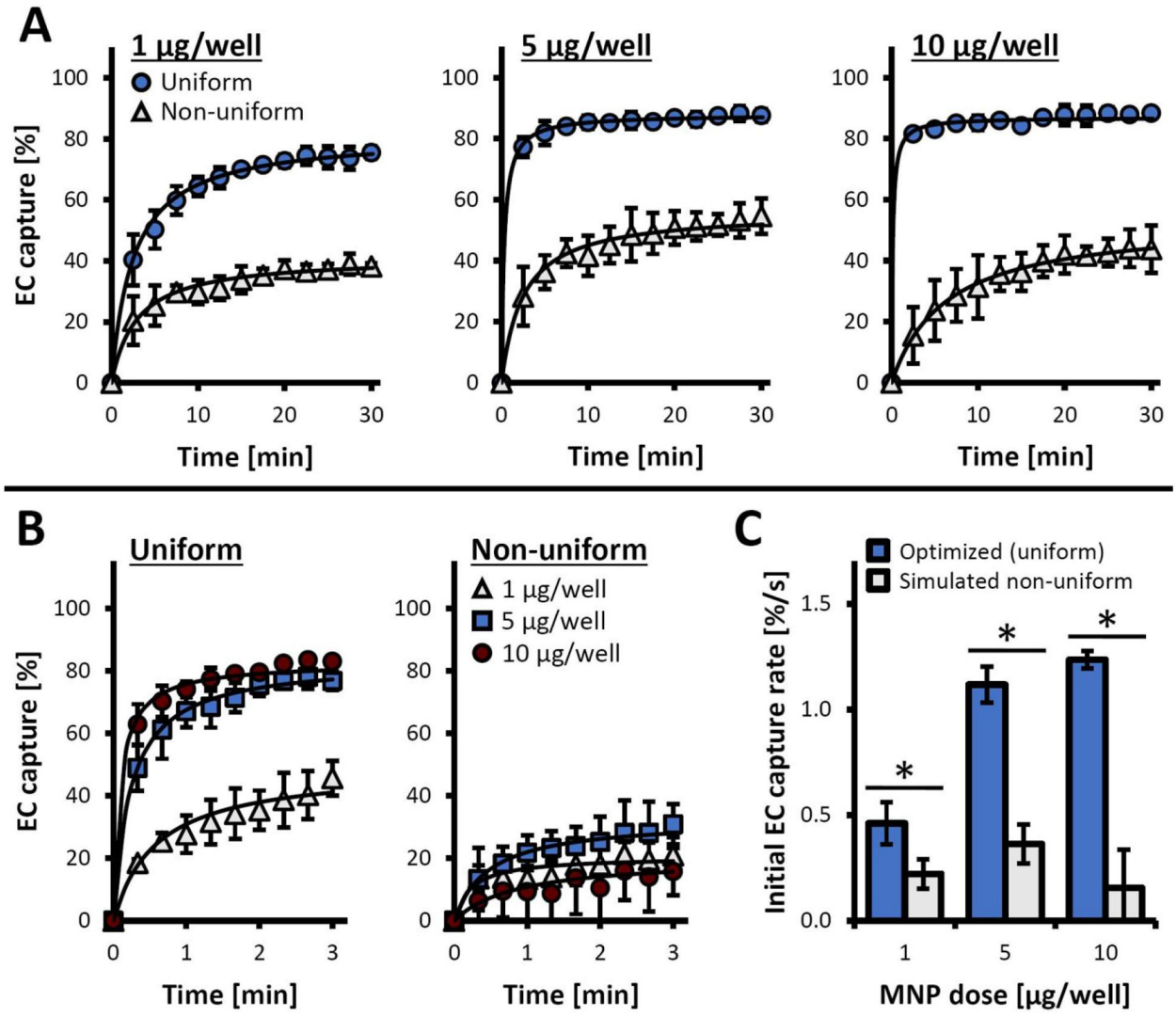

Figure 5.

EC capture using a depletion-based magnetophoresis assay. MNP-loaded EC were labeled with 3,3-dioctadecyloxacarbocyanine perchlorate and the fluorescence intensity of the EC suspensions were monitored longitudinally ($\lambda_{ex}/\lambda_{em}$ = 485 nm/535 nm) during exposure to a high-gradient magnetic field. (**A**) The time courses of fluorescence intensity changes are shown for EC loaded using 1, 5, and 10 µg MNP/well using the optimized (uniform) *vs.* simulated non-uniform loading procedures. Data are presented as normalized fluorescence intensities normalized to initial values (I_t/I_0). (**B**) The time course of cell capture shown in detail for the initial 3 min of the capture experiment: a comparison between EC loaded uniformly *vs.* non-uniformly with 1, 5, and 10 µg MNP/well. (**C**) Initial kinetics of cell capture (measured over the first minute), presented as fractional cell depletion per second for EC loaded uniformly *vs.* non-uniformly with 1, 5, and 10 µg MNP/well. An * denotes a statistically significant difference between the optimized (uniform) loading and the simulated, non-uniform loading procedures at a given MNP dose.